

Are your **MRI contrast agents** cost-effective?

Learn more about generic **Gadolinium-Based Contrast Agents**.



**AJNR**

## **A Review of Magnetic Particle Imaging and Perspectives on Neuroimaging**

L.C. Wu, Y. Zhang, G. Steinberg, H. Qu, S. Huang, M. Cheng, T. Bliss, F. Du, J. Rao, G. Song, L. Pisani, T. Doyle, S. Conolly, K. Krishnan, G. Grant and M. Wintermark

This information is current as of April 20, 2024.

*AJNR Am J Neuroradiol* 2019, 40 (2) 206-212

doi: <https://doi.org/10.3174/ajnr.A5896>

<http://www.ajnr.org/content/40/2/206>

# A Review of Magnetic Particle Imaging and Perspectives on Neuroimaging

 L.C. Wu,  Y. Zhang,  G. Steinberg,  H. Qu,  S. Huang,  M. Cheng,  T. Bliss,  F. Du,  J. Rao,  G. Song,  L. Pisani,  T. Doyle,  S. Conolly,  K. Krishnan,  G. Grant, and  M. Wintermark



## ABSTRACT

**SUMMARY:** Magnetic particle imaging is an emerging tomographic technique with the potential for simultaneous high-resolution, high-sensitivity, and real-time imaging. Magnetic particle imaging is based on the unique behavior of superparamagnetic iron oxide nanoparticles modeled by the Langevin theory, with the ability to track and quantify nanoparticle concentrations without tissue background noise. It is a promising new imaging technique for multiple applications, including vascular and perfusion imaging, oncology imaging, cell tracking, inflammation imaging, and trauma imaging. In particular, many neuroimaging applications may be enabled and enhanced with magnetic particle imaging. In this review, we will provide an overview of magnetic particle imaging principles and implementation, current applications, promising neuroimaging applications, and practical considerations.

**ABBREVIATIONS:** FFL = field-free line; FFP = field-free point; FFR = field-free region; MPI = magnetic particle imaging; SPIO = superparamagnetic iron oxide; SPION = superparamagnetic iron oxide nanoparticle

Magnetic particle imaging (MPI) is a new tomographic technique developed in the early 2000s.<sup>1</sup> In contrast to traditional imaging modalities such as MR imaging, sonography, x-ray, and CT, MPI is not a structural imaging technique. Instead, it is a tracer imaging technique similar to PET and SPECT. MPI allows tracking and quantification of tracer materials, specifically magnetic nanoparticles. It is a quantitative 3D imaging technique with high spatial and high temporal resolution, which may allow real-time high-resolution in vivo imaging. Prototype scanners and, more recently, commercial animal scanners have yielded the first in vivo MPI studies demonstrating applications in vascular imaging,<sup>2-4</sup> oncology,<sup>5-7</sup> and cell-tracking.<sup>8,9</sup> Human scanners are being developed and will become available in a few years. As an

emerging imaging technique, MPI may open up new possibilities in 3D in vivo real-time imaging.

In this review, we will introduce the principles and applications of MPI for researchers and clinicians in the neuroimaging field. We will start with a basic description of the physics and construction of MPI, then talk more in depth about the current applications and discuss promising neuroimaging applications. We will also include practical considerations and comparisons with other imaging modalities for reference.


## Magnetic Particle Imaging Principles

**MPI Physics.** MPI uses a magnetic gradient field, known as a selection field, to saturate all superparamagnetic iron oxide (SPIO) magnetization outside a central field-free region, known as a field-free point (FFP) or field-free line (FFL). The FFL is rapidly shifted over an imaging volume via a rapidly varying excitation/drive field to produce an image. Large fields of view are traversed using slower shift fields and mechanical translation. To produce a signal, as the FFL traverses a SPION's location, the SPION's magnetization changes nonlinearly in response. This time-varying magnetization induces a voltage in the receiver coil, which can be assigned to the instantaneous FFL location to produce a magnetic particle image. The voltages induced are linearly proportional to the number of SPIONs at the instantaneous FFL location, enabling quantification of SPIONs. Most importantly, biologic tissue does not generate or attenuate the low-frequency magnetic fields used in MPI, giving the technique ideal contrast


Received April 23, 2018; accepted after revision July 6.

From the Departments of Bioengineering (L.C.W.), Neurosurgery (G.S., M.C., T.B., F.D., G.G.), Radiology (Y.Z., H.Q., S.H., M.W.), Neuroradiology Section, Radiology (J.R., G.S., L.P.), and Pediatrics (T.D.), Stanford University, Stanford, California; Department of Electrical Engineering and Computer Sciences (S.C.), University of California Berkeley, Berkeley, California; Departments of Materials Sciences and Engineering and Physics (K.K.), University of Washington, Seattle, Washington; and Chongqing Medical University (S.H.), Traditional Chinese Medicine College, Chongqing, China.

Please address correspondence to Max Wintermark, MD, Stanford University School of Medicine, Department of Radiology, Neuroradiology Section, 300 Pasteur Dr, Grant S047, Stanford, CA 94305; e-mail: max.wintermark@gmail.com

 Indicates open access to non-subscribers at [www.ajnr.org](http://www.ajnr.org)

 Indicates article with supplemental on-line appendix.

 Indicates article with supplemental on-line photos.

<http://dx.doi.org/10.3174/ajnr.A5896>

**Comparison of MPI with common clinical imaging modalities<sup>21–25</sup>**

Modality	Ultrasound	CT	MRI	PET	SPECT	MPI
Main clinical applications	Structural imaging	Structural imaging	Structural imaging	Tracer imaging	Tracer imaging	Tracer imaging
Spatial resolution	1 mm	<1 mm	1 mm	4 mm	3–10 mm	1 mm
Temporal resolution	<1 second	Seconds	Seconds to hours	Minutes	Minutes	<1 second to minutes
Contrast agents/tracers	Microbubbles	Iodine	Gadolinium, iron oxide particles	Radioactive tracers	Radioactive tracers	Iron oxide particles
Sensitivity	Low	Low	Low	High	High	High
Patient risk	Heating and cavitation	Radiation	Heating and peripheral nerve stimulation	Radiation	Radiation	Heating and peripheral nerve stimulation
Cost	Low	Medium	High	High	Medium	Medium

independent of the source depth. These fields are further described in the On-line Appendix.

### Scanner Construction

The magnetic fields required for MPI are very different from those used in MR imaging, so MPI scans cannot be acquired on a standard MR imaging scanner. A magnetic particle imager has 3 major components: The main magnet subsystem generates the main magnetic field gradient and shifts the field-free region (FFR) to cover the full FOV, the transmit/receive subsystem generates the drive field and receives the signal produced by the nanoparticles, and the control console coordinates operation of the major subsystems and processes the received signal to produce an image.<sup>10</sup> Typically, the main magnet produces both the selection field and the slow-shift fields, driving the native resolution of the system. The drive coils in the transmit/receive subsystem generate the excitation signals in the nanoparticles, and this subsystem is designed for decoupling much lower nanoparticle signals from the excitation/drive signal. These MPI scanner components are further described in the On-line Appendix.

### Resolution, Contrast, and Sensitivity

The Table provides a comparison of MPI with common clinical imaging modalities. The resolution of the technique is driven by the interaction of the nanoparticle and the gradient.<sup>11–13</sup> This drives the native resolution of the system, which can be expressed as full width at half maximum.<sup>13</sup> For stronger gradient strengths such as 6.1 T/m used in a MOMENTUM system (Magnetic Insight, Alameda, California), tailored nanoparticles have been demonstrated to have ~700- $\mu$ m full width at half maximum resolution, and point sources remain distinguishable at a 600- $\mu$ m separation.<sup>14</sup> While the native resolution of a system derives only from interaction of the gradient and nanoparticle, there are numerous techniques for improving the visual quality of the images by trading the SNR of the technique for image resolution.<sup>15</sup> These techniques are frequently used in MPI to good effect and can appreciably improve resolution for lower systems with lower gradient strengths.<sup>15</sup> The resolution compares well with clinical nuclear medicine. For example, clinical PET cameras have a fundamental resolution limit of ~2 mm, with a practical resolution limit of ~2.5 mm,<sup>16</sup> and typically SPECT has a resolution of ~10 mm,<sup>17</sup> though some systems have a resolution as fine as 3 mm (eg, G-SPECT; MILabs, Utrecht, the Netherlands).

The contrast and signal to noise ratio is excellent with MPI because MPI sees only a tracer and does not see tissue. More specifically, MPI is not affected by the endogenous iron present in the body: It can see only injected SPIONs. This is similar to PET and SPECT, which also have no background signal from tissue. However, PET and SPECT, with imaging times on the order of minutes, are not suited for dynamic imaging applications. PET and SPECT tracers also have half-lives on the order of minutes to hours, while MPI tracers can last for days to weeks.<sup>18</sup> MPI contrast shows the greatest benefits in techniques in which the high contrast can lead to higher accuracy, such as perfusion imaging and cell tracking. This benefit compares favorably with traditional structural imaging techniques such as MR imaging and CT, which can struggle to produce reliable perfusion imaging.<sup>19</sup>

The sensitivity of the technique is because MPI directly detects the electronic magnetization of iron oxide nanoparticles, a magnetization that is large compared with the nuclear magnetization detected in MR imaging.<sup>20</sup> This feature gives MPI a low detection limit, meaning that minute amounts of tracer material can be detected. For example, the iron detection limit was 1.1 ng (SNR = 3.9) in a voxel of tailored MPI tracers using a high-sensitivity FFL scanner with a 5.7-T/m gradient with a native resolution of 800- $\mu$ m full width at half maximum.<sup>14</sup> The system was also used to detect dilute tracer (550 pg Fe/ $\mu$ L), which could be seen with SNR = 4.9.<sup>14</sup> As MPI systems begin to mature, their sensitivity should continue to improve. Current systems have limits as low as ~200 cells in a voxel,<sup>9,18</sup> and theoretically, the MPI detection limit may be as little as 1–10 iron oxide cells in a voxel.<sup>18</sup>

### Applications of MPI and Perspectives on Neuroimaging

**Vascular Imaging.** Currently the standard of care for cerebral blood perfusion imaging is CT perfusion, which poses ionizing radiation risks. MPI is well-suited for measuring perfusion. A study demonstrated imaging of cerebral blood flow in living mice using MPI.<sup>2</sup> This was followed by a demonstration of MPI perfusion in mice for imaging stroke.<sup>3</sup> In our work, we recently measured CBV and CBF in a rat.<sup>4</sup> In addition, we performed in vivo cerebral blood perfusion in stroke mice with MPI (Fig 1), in which an intravenous bolus of iron nanoparticles was administered to mice. Tomographic 3D-MPI was performed using a MOMENTUM MPI system (Magnetic Insight). We

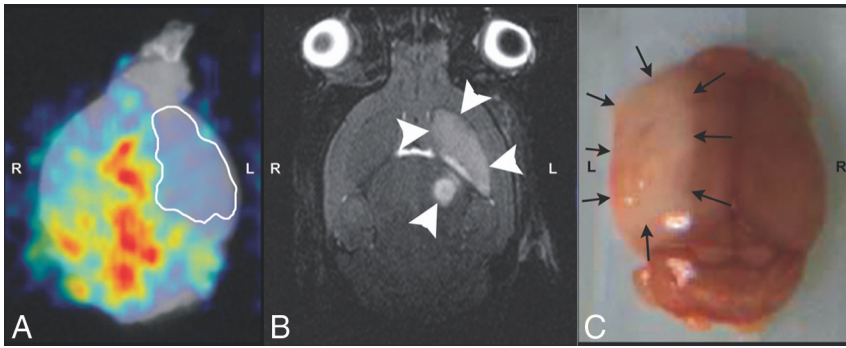


**FIG 1.** Perfusion, structural, and histology images from a mouse injected with the nanoparticles. The parameters were the following: FOV = 4 cm, 35 projections, best image quality, Lodespin scan mode. A 70- to 100- L intravenous bolus of iron nanoparticles (0.949 mg Fe/mL; core diameter, 27.6 nm) donated by Dr Kannan Krishnan, University of Washington, was administered to C57Bl/6 stroke mice through tail veins. The mice were sacrificed within 30 minutes postinjection, and 3D-MPI was performed using a MOMENTUM MPI system. Anatomic images were collected on the eXplore CT-120 microCT (GE Healthcare, Milwaukee, Wisconsin) and a 7T MR imaging scanner (BioSpec; Bruker Instruments, Billerica, Massachusetts). Data analysis and image registration were performed using the Horos (<https://sourceforge.net/projects/horos/>) and VivoQuant software (Invicro, Boston, Massachusetts). In vivo iron oxide quantification was performed by imaging fiducials containing a known concentration of tracer positioned beside the animal. A, In the 2D coregistered image from CT and MPI, the MPI signal (red if high, yellow if intermediate, blue if low) from the left hemisphere is less than that from the contralateral side (*red spots* indicate vascular structures with high blood volume). B, The high T2 signal (stroke lesion, *arrowheads*) in the left basal ganglia and thalamus. C, The histology image of a perfusion-fixed whole brain shows the stroke lesion on the left (L). R indicates right.

showed that lower MPI signal (a measure of CBV) is observed on the side of the brain with the stroke lesion.

Another promising application of MPI is to image vasculature. MPI provides 3D information, and the signal is directly related to blood volume in a vessel. This is an improvement over 2D techniques such as x-ray or DSA. CT or MR angiography, while providing 3D images, has background noise from the surrounding tissue and calcium, which is not a concern for MPI. In MPI, 3D angiography can be performed using bolus tracking or blood pool agents. An MPI-specific long circulating nanoparticle can repeatedly measure the blood pool with 1 single injection, enabling tracking of changes from minutes to hours.<sup>26</sup> For example, we recently demonstrated use of a long circulating tracer to detect gut bleed,<sup>27</sup> in which a transgenic mouse model with bleeding induced in the gut using heparin was imaged with 21 repeat MPI scans for 80 minutes. In another study in a rat model of traumatic brain injury, animals were monitored longitudinally to study cerebral bleeding caused by the impact. We showed differences in the nanoparticle clearance rate in different regions of the brain in the impacted animals compared with the controls over a 2-week period.<sup>28</sup>

MPI is also capable of very fast imaging, similar to x-ray and DSA, enabling tracking of fast blood flow dynamics. Previously, 1 study demonstrated 3D in vivo imaging of a beating mouse heart using a clinically approved concentration ( $<40 \mu\text{mol} [\text{Fe}] 1^{-1}$ ) of Resovist (ferucarbotran; Bayer Schering Pharma, Berlin, Germany), with a temporal resolution of 21.5 ms, FOV of 1–2 cm, and resolution sufficient to resolve heart chambers.<sup>29</sup> In addition, it has been shown that catheters and guidewires can be tracked with MPI, enabling image-guided interventions.<sup>30,31</sup>

**Oncology.** A promising application for MPI is in oncology. MPI could be used to image tumor vascularization, which may be im-

portant in indicating tumor stage and treatment efficacy. We recently demonstrated MPI visualization in a breast cancer xenograft model and showed that MPI can see both the early dynamic contrast-enhanced effect of nanoparticles flowing into a tumor, followed by the enhanced permeability and retention effect during the following 48 hours.<sup>32</sup>

In neuro-oncology, conventional MR imaging and CT lack reliability in assessing the size and location of brain tumors, and they are often not specific enough to differentiate tumor progression from other treatment-related changes.<sup>33,34</sup> While traditional PET for glucose metabolism is often used in peripheral tumor imaging, it cannot provide good contrast for brain tumors due to the high levels of glucose metabolism inherent in the brain, and novel tracers such as radio-labeled amino acids are required for better contrast.<sup>35</sup> MPI may provide a promising alternative, especially as brain-specific MPI tracers are

developed to improve specificity, enhance retention times, and reduce potential harm to the patient.

In brain tumor studies, SPION size can be optimized to passively target and accumulate in a brain tumor because the tumor is hypervascularized with leaky vessels while the blood-brain barrier blocks access to healthy brain tissue.<sup>36–38</sup> Active tumor targeting can also be achieved via surface chemistry modifications or the use of magnetic fields. For example, it was shown that lactoferrin-conjugated nanoparticles can be used to target brain glioma cells in MPI.<sup>5</sup> By means of a human glioblastoma mouse model, fluorescent magnetic nanoparticles could be magnetically retained in the neovasculature as well as tissue of the tumor, using a magnetic micromesh.<sup>6</sup>

MPI can also be used for sentinel lymph node imaging and hyperthermia treatment. The current state of the art is to use radioactive colloid tracers, which could be replaced with MPI tracers. This was demonstrated in a mouse cancer model,<sup>7</sup> in which magnetic tracer material was seen depositing in tumor tissue and/or sentinel lymph nodes near tumors. In hyperthermia treatment, magnetic particles injected into tumors can locally heat the tissue around the FFR. It was demonstrated that the MPI-measured magnetic particle concentration correlated well with tumor volume decrease after magnetic hyperthermia.<sup>39</sup> In another study, it was shown that magnetic nanofibers loaded with magnetic nanoparticles could be visualized using MPI and used for magnetic hyperthermia.<sup>40</sup>

**Cell Labeling and Tracking.** MPI is promising for cell tracking because the technique is independent of depth in tissue with millimeter-scale resolution, robust linear quantification, and high sensitivity. We evaluated MPI for tracking of systemically administered mesenchymal stem cells.<sup>8</sup> Mesenchymal stem cells are of



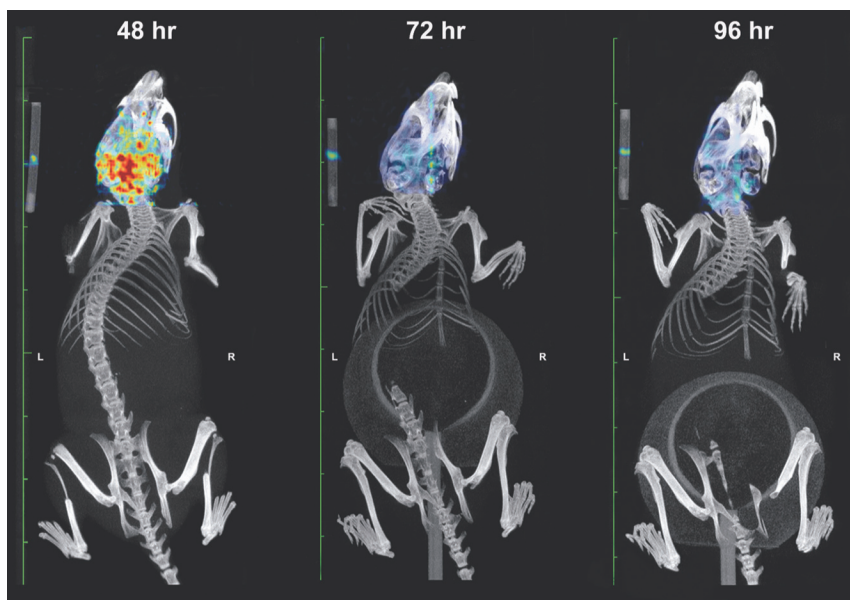


**FIG 2.** SPION-labeled macrophages have long retention times in the brain of a stroke mouse. We administered  $1\text{--}2 \times 10^6$  nanoparticle (VivoTrax; Magnetic Insight)-labeled mouse macrophages (Raw 264.7; American Type Culture Collection, Manassas, Virginia) to BALB/c mice through tail veins 24 hours after stroke. At 48, 72, and 96 hours poststroke, 2D-MPI was performed using a MOMENTUM MPI system. The MPI protocol used the parameters of FOV = 4 cm, 55 projections, best image quality, and default scan mode. Anatomic images were collected on the eXplore CT-120 microCT. Data analysis and image registration were performed using the Horos and VivoQuant software. In vivo iron oxide quantification was performed by imaging a fiducial containing a known concentration of tracer positioned beside the animal. The MPI signal was detected in the brain at 48, 72, and 96 hours poststroke; the accumulation of iron-labeled cells was the highest at 48 hours and reduced with time.

particular therapeutic interest because they can control inflammation and modify the proliferation and cytokine production of immune cells.<sup>41</sup> Intravenous injections are sometimes used to deliver mesenchymal stem cells in both animal models and clinical trials.<sup>42,43</sup> Our proof-of-concept study confirmed that >80% of mesenchymal stem cells are entrapped in pulmonary vasculature following intravenous injection.<sup>8</sup> In a different study, it was shown that rat and human adult stem cells can uptake SPIONS and they localize in the cytoplasm.<sup>44</sup> Blood cell tracking is another application for MPI as a method for increasing circulation time.<sup>45</sup> Using red blood cells as the carriers also has the advantage of being able to increase circulation time from minutes to hours.<sup>2,46,47</sup> Additionally, there is ongoing work on the development of MPI-tailored nanoparticles, which can be functionalized for efficient targeting and cell labeling. We recently demonstrated that Janus nanoparticles made by encapsulating iron oxide nanoparticles in semiconducting polymers allowed efficient cell labeling and were sensitive enough to track 250 labeled HeLa cells after implantation in mice.<sup>9</sup>

These cell-labeling and tracking methods may also be applied to neuroimaging. In one study, it was shown that neural grafts could be monitored in rats. This study implanted neural progenitor cells into the forebrain of rats and measured nonsignificant signal decay during 87 days.<sup>18</sup> The authors demonstrated a detection sensitivity of <1000 cells in a voxel. As commercial development continues, we estimate that the theoretic detection limit may approach as little as 1–10 cells in a voxel. For comparison, these numbers compare favorably with MR imaging, in which the

first clinical cell-tracking detection limit was 15,000 cells.<sup>48</sup> In a preliminary experiment, we administered SPION-labeled mouse macrophages to stroke mice to test the localization and retention of signals for stroke monitoring (Fig 2). We showed that while the accumulation of iron-labeled cells was highest at 48 hours, there was still detectable MPI signal at 96 hours postinjection.

**Inflammation Tracking.** Inflammation is involved in many disease processes, including immune disorders, neurologic/neuropsychological disorders, and cancer. Detection and tracking of inflammation could help with diagnosis and monitor treatment outcomes. Unfortunately, current practices in tracking inflammation often involve biopsies or imaging methods that have low specificity and quantifiability. MPI may be a promising quantitative imaging alternative. Previous studies have already shown the use of SPIO tracers to target inflammation. SPIOs may be injected intravenously and may be taken up at inflammation sites, such as by macrophages at active phagocytic sites<sup>49,50</sup> or by atherosclerotic plaques.<sup>51,52</sup> Previous studies have used MR imaging to detect

the SPIONS for inflammation tracking.<sup>49,50,53,54</sup> However, with high magnetic susceptibility, SPIOs cause a decrease in signal intensity, which could often be confused with signal voids from bone, air bubbles, susceptibility blowouts, and imaging artifacts. With the use of MPI, SPIONS can be more specifically detected with a higher signal-to-noise ratio.

**Contrast Agent.** SPIO contrast agents have previously been developed for MR imaging contrast enhancement. SPIOs are relatively safe for the patient and are biodegradable through the reticuloendothelial system.<sup>55</sup> As mentioned previously, SPIO agents can achieve long retention times in the body up to hours or days when loaded into cells. In PET or SPECT, the radioactive tracers have shorter half-lives in the body, especially for the high-energy probes required in PET. In addition, due to the short half-life of PET tracers, PET requires a cyclotron on site. In comparison, the SPIOs used in MPI are much more stable and have longer shelf lives with lower production cost.<sup>56</sup> There are a number of commercial SPIO agents that have either received FDA approval or are in a clinical trial phase<sup>57</sup> to serve as potential contrast agents for MPI.<sup>58–61</sup> SPIONS have historically been used in humans as MR imaging contrast agents, and 2 tracers, ferucarbotran (Resovist) and ferumoxytol, remain on the market in the European Union/Asia Pacific and the United States/European Union/Asia Pacific, respectively. These agents have been approved for contrast-enhanced MR imaging of the liver/spleen.<sup>62,63</sup> MR imaging contrast agents can also be used for MPI. Additionally,

development and synthesis of MPI-tailored contrast agents are an emerging and important field of research.

MPI performance is affected by particle size, size distribution, relaxation properties, surface chemistry, and the environment.<sup>61,64–66</sup> MPI tracer development has so far been dominated by optimizing for particle core size and size distribution. This is especially important for MPI because particle size directly affects image resolution. We have shown that single-core tracers with core diameters of 26–27 nm provide excellent performance for MPI, and modeling studies predict 25–30 nm as the optimal diameter for iron oxide magnetic nanoparticles, with improved performance for uniform size and optimized magnetic properties.<sup>67,68</sup> Early research also shows that there is an optimal core size for each operating frequency that is driven by transition of the dominant relaxation effect from Néel to Brownian.<sup>67,68</sup> Additionally, for in vivo applications, further considerations need to be made for circulation time, biodistribution, and cellular uptake. Thus, new contrast agents more specifically targeted for MPI applications are being actively developed. These new particles are optimized for size and size distributions,<sup>68,69</sup> quality of crystal structure,<sup>9</sup> mass sensitivity,<sup>67</sup> high stability,<sup>70</sup> rich harmonic spectrum,<sup>71</sup> and surface chemistry.<sup>72–74</sup>

**Safety Considerations.** The current consensus is that MPI is safe to scale to human sizes. The primary concerns for MPI are the safety of the SPIONs and the safety of the time-varying magnetic fields. SPIONs are considered a low risk to patients and are well-tolerated, with some exceptions. First, large concentrations can lead to decreased cell proliferation.<sup>75</sup> Second, there have been some cases of moderate-to-severe allergic reactions to injections of SPIONs.<sup>76–78</sup>

There is comparatively less risk in the magnetic fields used by MPI, which is governed by the same limits to peripheral nerve stimulation and specific absorption rate that are seen in MR imaging. In a human subject study, it was found that the safe limit for peripheral nerve stimulation and the specific absorption rate in the chest is about 7 mT, between 25 and 50 kHz.<sup>79</sup> Cardiac stimulation and peripheral nerve stimulation will not be a limitation for clinical MPI systems.<sup>79–81</sup> In addition, for applications in which guidewires and catheters are used, heating of the equipment is also a potential concern.<sup>82</sup>

**Practical Considerations.** The hardware complexity of MPI is comparable with that of MR imaging. One of the difficult engineering tasks is while MR imaging requires a parts-per-million accurate main magnetic field, MPI requires a parts-per-million accurate sinusoidal drive field.<sup>83</sup> Both techniques require real-time control of magnetic fields and involve pulse sequences and reconstruction algorithms. In contrast to MR imaging, however, MPI scanning and imaging are straightforward, and we have not found that specialized training is required to acquire or interpret MPI. MPI contrast agents are widely available, easy to handle, and less expensive than commonly used radioactive probes. Like nuclear medicine, it can be helpful to have structural information with which to overlay MPI, and we frequently coregister MPI with CT and MR imaging. Thus, construction of hybrid systems to ease coregistration with anatomic images may be desirable in the future.

## CONCLUSIONS

MPI is a novel, promising imaging technique for sensitive, quantitative, and high-resolution in vivo imaging. Preliminary animal studies have shown promising applications, including vascular imaging, oncology imaging, cell tracking, and inflammation imaging. Much development work is being done to further improve imager design, tracer design, and imaging protocols. With these improvements and the upcoming development of human-sized scanners, MPI has the potential to become a widely adopted clinical tool for neuroimaging.

## ACKNOWLEDGMENTS

We would like to thank Anna Christensen, Patrick Goodwill, Jeff Gaudet, and Prachi Pandit from Magnetic Insight (<https://www.magneticinsight.com/>) and Daniel Smerin for their support in conducting our experiments.

Disclosures: Gary Steinberg—UNRELATED: Royalties: Peter Lazić US; Stock/Stock Options: Qool Therapeutics, NeuroSave. Comments: stock options only from both companies. Tim Doyle—UNRELATED: Payment for Lectures Including Service on Speakers Bureaus: Magnetic Insight, Comments: talk presented at a magnetic particle imaging workshop at the 2017 World Molecular Imaging Congress (Philadelphia). Honorarium was paid. Steven Conolly—UNRELATED: Grants/Grants Pending: National Institutes of Health, University of California, Office of the President.\* Max Wintermark—UNRELATED: Board Membership: GE NFL Advisory Board; Stock/Stock Options: MORE Health, Icometrix; Other: Equity, Comments: Magnetic Insight. Kannan Krishnan—UNRELATED: Grant: University of Washington.\* \*Money paid to the institution.

## REFERENCES

1. Gleich B, Weizenecker J. **Tomographic imaging using the nonlinear response of magnetic particles.** *Nature* 2005;435:1214–17 CrossRef Medline
2. Rahmer J, Gleich B, Weizenecker J, et al. **3D real-time magnetic particle imaging of cerebral blood flow in living mice.** In: *Proceedings of the International Society for Magnetic Resonance in Medicine*, 18, 2010
3. Ludewig P, Gdaniec N, Sedlacik J, et al. **Magnetic particle imaging for real-time perfusion imaging in acute stroke.** *ACS Nano* 2017;11:10480–88 CrossRef Medline
4. Orendorff R, Keselman K, Conolly S. **Quantitative cerebral blood flow and volume measurements by magnetic particle imaging.** In: *13th European Molecular Imaging Meeting*, March 20–23, 2018. San Sebastián, Spain
5. Tomitaka A, Arami H, Gandhi S, et al. **Lactoferrin conjugated iron oxide nanoparticles for targeting brain glioma cells in magnetic particle imaging.** *Nanoscale* 2015;7:16890–98 CrossRef Medline
6. Fu A, Wilson RJ, Smith BR, et al. **Fluorescent magnetic nanoparticles for magnetically enhanced cancer imaging and targeting in living subjects.** *ACS Nano* 2012;6:6862–69 CrossRef Medline
7. Finas D, Baumann K, Sydow L, et al. **Lymphatic tissue and superparamagnetic nanoparticles: magnetic particle imaging for detection and distribution in a breast cancer model.** *Biomed Tech* 2013 Sep 7. [Epub ahead of print] CrossRef Medline
8. Zheng B, von See MP, Yu E, et al. **Quantitative magnetic particle imaging monitors the transplantation, biodistribution, and clearance of stem cells in vivo.** *Theranostics* 2016;6:291–301 CrossRef Medline
9. Song G, Chen M, Zhang Y, et al. **Janus iron oxides @ semiconducting polymer nanoparticle tracer for cell tracking by magnetic particle imaging.** *Nano Lett* 2018;18:182–89 CrossRef Medline
10. Goodwill PW, Lu K, Zheng B, et al. **An x-space magnetic particle imaging scanner.** *Rev Sci Instrum* 2012;83 CrossRef Medline
11. Rahmer J, Weizenecker J, Gleich B, et al. **Signal encoding in magnetic particle imaging: properties of the system function.** *BMC Med Imaging* 2009;9:4 CrossRef Medline

12. Goodwill PW, Conolly SM. **The X-space formulation of the magnetic particle imaging process: 1-D signal, resolution, bandwidth, SNR, SAR, and magnetostimulation.** *IEEE Trans Med Imaging* 2010; 29:1851–59 CrossRef Medline
13. Goodwill PW, Conolly SM. **Multidimensional X-space magnetic particle imaging.** *IEEE Trans Med* 2011;30:1581–90 CrossRef
14. Arami H, Teeman E, Troksa A, et al. **Tomographic magnetic particle imaging of cancer targeted nanoparticles.** *Nanoscale* 2017;9: 18723–30 CrossRef Medline
15. Knopp T, Biederer S, Sattel TF, et al. **Prediction of the spatial resolution of magnetic particle imaging using the modulation transfer function of the imaging process.** *IEEE Trans Med Imaging* 2011;30: 1284–92 CrossRef Medline
16. Moses WW. **Fundamental limits of spatial resolution in PET.** *Nucl Instrum Methods Phys Res A* 2011;648(Supplement 1):S236–40 CrossRef Medline
17. Bailey DL, Willowson KP. **An evidence-based review of quantitative SPECT imaging and potential clinical applications.** *J Nucl Med* 2013;54:83–89 CrossRef Medline
18. Zheng B, Vazin T, Goodwill PW, et al. **Magnetic particle imaging tracks the long-term fate of in vivo neural cell implants with high image contrast.** *Sci Rep* 2015;5:14055 CrossRef Medline
19. Wintermark M, Sesay M, Barbier E, et al. **Comparative overview of brain perfusion imaging techniques.** *Stroke* 2005;36:83–99 CrossRef Medline
20. Saritas EU, Goodwill PW, Croft LR, et al. **Magnetic particle imaging (MPI) for NMR and MRI researchers.** *J Magn Reson* 2013;229: 116–26 CrossRef Medline
21. Knopp T, Buzug TM. *Magnetic Particle Imaging: An Introduction to Imaging Principles and Scanner Instrumentation.* Heidelberg: Springer-Verlag; 2012
22. Kherlopian AR, Song T, Duan Q, et al. **A review of imaging techniques for systems biology.** *BMC Syst Biol* 2008;2:74 CrossRef Medline
23. Weissleder R. **Scaling down imaging: molecular mapping of cancer in mice.** *Nat Rev Cancer* 2002;2:11–18 CrossRef Medline
24. Cox B, Beard P. **Imaging techniques: super-resolution ultrasound.** *Nature* 2015;527:451–52 CrossRef Medline
25. Goodwill PW, Saritas EU, Croft LR, et al. **X-space MPI: magnetic nanoparticles for safe medical imaging.** *Adv Mater* 2012;24:3870–77 CrossRef Medline
26. Khandhar AP, Keselman P, Kemp SJ, et al. **Evaluation of PEG-coated iron oxide nanoparticles as blood pool tracers for preclinical magnetic particle imaging.** *Nanoscale* 2017;9:1299–306 CrossRef Medline
27. Yu EY, Chandrasekharan P, Berzon R, et al. **Magnetic particle imaging for highly sensitive, quantitative, and safe in vivo gut bleed detection in a murine model.** *ACS Nano* 2017;11:12067–76 CrossRef Medline
28. Orendorff R, Peck AJ, Zheng B. **First in vivo traumatic brain injury imaging via magnetic particle imaging.** *Phys Med Biol* 2017;62: 3501–09 CrossRef Medline
29. Weizenecker J, Gleich B, Rahmer J, et al. **Three-dimensional real-time in vivo magnetic particle imaging.** *Phys Med Biol* 2009;54: L1–10 CrossRef Medline
30. Haegele J, Biederer S, Wojtczyk H, et al. **Toward cardiovascular interventions guided by magnetic particle imaging: first instrument characterization.** *Magn Reson Med* 2013;69:1761–67 CrossRef Medline
31. Haegele J, Rahmer J, Gleich B, et al. **Magnetic particle imaging: visualization of instruments for cardiovascular intervention.** *Radiology* 2012;265:933–38 CrossRef
32. Yu EY, Bishop M, Zheng B, et al. **Magnetic particle imaging: a novel in vivo imaging platform for cancer detection.** *Nano Lett* 2017;17: 1648–54 CrossRef Medline
33. Ryken TC, Aygun N, Morris J, et al. **The role of imaging in the management of progressive glioblastoma: a systematic review and evidence-based clinical practice guideline.** *J Neurooncol* 2014;118: 435–60 CrossRef Medline
34. Verma N, Cowperthwaite MC, Burnett MG, et al. **Differentiating tumor recurrence from treatment necrosis: a review of neuro-oncologic imaging strategies.** *Neuro Oncol* 2013;15:515–34 CrossRef Medline
35. Langen KJ, Watts C. **Neuro-oncology: amino acid PET for brain tumors—ready for the clinic?** *Nat Rev Neurol* 2016;12:375–76 CrossRef Medline
36. Maeda H, Wu J, Sawa T, et al. **Tumor vascular permeability and the EPR effect in macromolecular therapeutics: a review.** *J Control Release* 2000;65:271–84 CrossRef Medline
37. Béduneau A, Saulnier P, Benoit JP. **Active targeting of brain tumors using nanocarriers.** *Biomaterials* 2007;28:4947–67 CrossRef Medline
38. Cheng Y, Morshed RA, Auffinger B, et al. **Multifunctional nanoparticles for brain tumor imaging and therapy.** *Adv Drug Deliv Rev* 2014;66:42–57 CrossRef Medline
39. Murase K, Aoki M, Banura N, et al. **Usefulness of magnetic particle imaging for predicting the therapeutic effect of magnetic hyperthermia.** *Open Journal of Medical Imaging* 2015;5:85–99 CrossRef
40. Murase K, Mimura A, Banura N, et al. **Visualization of magnetic nanofibers using magnetic particle imaging.** *Open Journal of Medical Imaging* 2015;05:56–65 CrossRef
41. Eggenhofer E, Luk F, Dahlke MH, et al. **The life and fate of mesenchymal stem cells.** *Front Immunol* 2014;5:148 CrossRef Medline
42. Wu Y, Zhao RC. **The role of chemokines in mesenchymal stem cell homing to myocardium.** *Stem Cell Rev* 2012;8:243–50 CrossRef Medline
43. Harting MT, Jimenez F, Xue H, et al. **Intravenous mesenchymal stem cell therapy for traumatic brain injury.** *J Neurosurg* 2009;110: 1189–97 CrossRef Medline
44. Lütke-Buzug K, Rapoport D. **Characterization of iron-oxide loaded adult stem cells for magnetic particle imaging in targeted cancer therapy.** *AIP Conf Proc* 2010;1311:244–48
45. Antonelli A, Sfara C, Rahmer J, et al. **Red blood cells as carriers in magnetic particle imaging.** *Biomed Tech (Berl)* 2013;58:517–25 CrossRef Medline
46. Markov DE, Boeve H, Gleich B, et al. **Human erythrocytes as nanoparticle carriers for magnetic particle imaging.** *Phys Med Biol* 2010; 55:6461–73 CrossRef Medline
47. Haegele J, Duschka R, Graeser M, et al. **Magnetic particle imaging: kinetics of the intravascular signal in vivo.** *Int J Nanomedicine* 2014; 9:4203–09 CrossRef Medline
48. de Vries IJ, Lesterhuis WJ, Barentsz JO, et al. **Magnetic resonance tracking of dendritic cells in melanoma patients for monitoring of cellular therapy.** *Nat Biotechnol* 2005;23:1407–13 CrossRef Medline
49. Lefevre S, Ruimy D, Jehl F, et al. **Septic arthritis: monitoring with USPIO-enhanced macrophage MR imaging.** *Radiology* 2011;258: 722–28 CrossRef Medline
50. Lutz AM, Weishaupt D, Persohn E, et al. **Imaging of macrophages in soft-tissue infection in rats: relationship between ultrasmall superparamagnetic iron oxide dose and MR signal characteristics.** *Radiology* 2005;234:765–75 CrossRef Medline
51. Ruehm SG, Corot C, Vogt P, et al. **Magnetic resonance imaging of atherosclerotic plaque with ultrasmall superparamagnetic particles of iron oxide in hyperlipidemic rabbits.** *Circulation* 2001;103: 415–22 CrossRef Medline
52. Sigovan M, Bousset L, Sulaiman A, et al. **Rapid-clearance iron nanoparticles for inflammation imaging of atherosclerotic plaque: initial experience in animal model.** *Radiology* 2009;252:401–09 CrossRef Medline
53. Metz S, Beer AJ, Settles M, et al. **Characterization of carotid artery plaques with USPIO-enhanced MRI: assessment of inflammation and vascularity as in vivo imaging biomarkers for plaque vulnerability.** *Int J Cardiovasc Imaging* 2011;27:901–12 CrossRef Medline
54. McAteer MA, Sibson NR, von Zur Muhlen C, et al. **In vivo magnetic resonance imaging of acute brain inflammation using microparticles of iron oxide.** *Nat Med* 2007;13:1253–58 CrossRef Medline
55. Wang YX. **Superparamagnetic iron oxide based MRI contrast agents: current status of clinical application.** *Quant Imaging Med Surg* 2011;1:35–40 CrossRef Medline
56. Panagiotopoulos N, Duschka RL, Ahlborg M, et al. **Magnetic particle**



- imaging: current developments and future directions.** *Int J Nano-medicine* 2015;10:3097–114 CrossRef Medline
57. Wang YX, Hussain SM, Krestin GP. **Superparamagnetic iron oxide contrast agents: physicochemical characteristics and applications in MR imaging.** *Eur Radiol* 2001;11:2319–31 CrossRef Medline
  58. Bonnemain B. **Superparamagnetic agents in magnetic resonance imaging: physicochemical characteristics and clinical applications—a review.** *J Drug Target* 1998;6:167–74 CrossRef Medline
  59. Sun C, Lee JS, Zhang M. **Magnetic nanoparticles in MR imaging and drug delivery.** *Adv Drug Deliv Rev* 2008;60:1252–65 CrossRef Medline
  60. Pablico-Lansigan MH, Situ SF, Samia AC. **Magnetic particle imaging: advancements and perspectives for real-time in vivo monitoring and image-guided therapy.** *Nanoscale* 2013;5:4040–55 CrossRef Medline
  61. Bauer LM, Situ SF, Griswold MA, et al. **Magnetic particle imaging tracers: state-of-the-art and future directions.** *J Phys Chem Lett* 2015;6:2509–17 CrossRef Medline
  62. Reimer P, Tombach B. **Hepatic MRI with SPIO: detection and characterization of focal liver lesions.** *Eur Radiol* 1998;1204:1198–204 CrossRef Medline
  63. Reimer P, Balzer T. **Ferucarbotran (Resovist): a new clinically approved RES-specific contrast agent for contrast-enhanced MRI of the liver—properties, clinical development, and applications.** *Eur Radiol* 2003;13:1266–76 CrossRef Medline
  64. Eberbeck D, Wiekhorst F, Wagner S, et al. **How the size distribution of magnetic nanoparticles determines their magnetic particle imaging performance.** *Appl Phys Lett* 2011;98:182502 CrossRef
  65. Khandhar AP, Ferguson RM, Arami H, et al. **Tuning surface coatings of optimized magnetite nanoparticle tracers for in vivo magnetic particle imaging.** *IEEE Trans Magn* 2015;51:395–401 CrossRef
  66. Arami H, Ferguson RM, Khandhar AP, et al. **Size-dependent ferrohydrodynamic relaxometry of magnetic particle imaging tracers in different environments.** *Med Phys* 2013;40:071904 CrossRef Medline
  67. Ferguson RM, Minard KR, Khandhar AP, et al. **Optimizing magnetite nanoparticles for mass sensitivity in magnetic particle imaging.** *Med Phys* 2011;38:1619–26 CrossRef Medline
  68. Ferguson RM, Minard KR, Krishnan KM. **Optimization of nanoparticle core size for magnetic particle imaging.** *J Magn Magn Mater* 2009;321:1548–51 CrossRef Medline
  69. Ferguson RM, Khandhar AP, Krishnan KM. **Tracer design for magnetic particle imaging (invited).** *J Appl Phys* 2012;07B318 CrossRef
  70. Arami H, Krishnan KM. **Highly stable amine functionalized iron oxide nanoparticles designed for magnetic particle imaging (MPI).** *IEEE Trans Magn* 2013;49:3500–03 CrossRef
  71. Ludwig F, Wawrzik T, Yoshida T, et al. **Optimization of magnetic nanoparticles for magnetic particle imaging.** *IEEE Trans Magn* 2012;48:3780–83 CrossRef
  72. Starmans LW, Burdinski D, Haex NP, et al. **Iron oxide nanoparticle-micelles (ION-micelles) for sensitive (molecular) magnetic particle imaging and magnetic resonance imaging.** *PLoS One* 2013;8:e57335 CrossRef Medline
  73. Starmans LW, Moonen RP, Aussems-Custers E, et al. **Evaluation of iron oxide nanoparticle micelles for magnetic particle imaging (MPI) of thrombosis.** *PLoS One* 2015;10:e0119257 CrossRef Medline
  74. Ishihara Y, Honma T, Nohara S, et al. **Evaluation of magnetic nanoparticle samples made from biocompatible ferucarbotran by time-correlation magnetic particle imaging reconstruction method.** *BMC Med Imaging* 2013;13:15 CrossRef Medline
  75. Lindemann A, Lütke-Buzug K, Fräderich BM, et al. **Biological impact of superparamagnetic iron oxide nanoparticles for magnetic particle imaging of head and neck cancer cells.** *Int J Nanomedicine* 2014;9:5025–40 CrossRef Medline
  76. Kehagias DT, Gouliamos AD, Smyrniotis V, et al. **Diagnostic efficacy and safety of MRI of the liver with superparamagnetic iron oxide particles (SH U 555 A).** *J Magn Reson Imaging* 2001;14:595–601 CrossRef Medline
  77. Bernd H, De Kerviler E, Gaillard S, et al. **Safety and tolerability of ultrasmall superparamagnetic iron oxide contrast agent: comprehensive analysis of a clinical development program.** *Invest Radiol* 2009;44:336–42 CrossRef Medline
  78. Singh A, Patel T, Hertel J, et al. **Safety of ferumoxytol in patients with anemia and CKD.** *Am J Kidney Dis* 2008;52:907–15 CrossRef Medline
  79. Saritas EU, Goodwill PW, Zhang GZ, et al. **Magnetostimulation limits in magnetic particle imaging.** *IEEE Trans Med Imaging* 2013;32:1600–10 CrossRef Medline
  80. Saritas EU, Goodwill PW, Zhang GZ, et al. **Safety limits for human-size magnetic particle imaging systems.** In: Buzug TM, Knopp T, eds. *Magnetic Particle Imaging*. Berlin: Springer-Verlag; 2011:325–30
  81. Schmale I, Gleich B, Rahmer J, et al. **MPI safety in the view of MRI safety standards.** *IEEE Trans Mag* 2015;51:1–4 CrossRef
  82. Duschka RL, Wojtczyk H, Panagiotopoulos N, et al. **Safety measurements for heating of instruments for cardiovascular interventions in magnetic particle imaging (MPI): first experiences.** *J Healthc Eng* 2014;5:79–93 CrossRef Medline
  83. Croft LR, Goodwill PW, Konkle JJ, et al. **Low drive field amplitude for improved image resolution in magnetic particle imaging.** *Med Phys* 2016;43:424 CrossRef Medline